

## Differential usage of carbohydrate co-receptors influences cellular tropism of Theiler's murine encephalomyelitis virus infection of the central nervous system

Howard L. Lipton · A.S. Manoj Kumar ·  
Shannon Hertzler · Honey V. Reddi

© Springer Science + Business Media, LLC 2006

**Abstract** Theiler's murine encephalomyelitis viruses (TMEV) are ubiquitous pathogens of mice, producing either rapidly fatal encephalitis (high-neurovirulence strains) or persistent central nervous system infection and inflammatory demyelination (low-neurovirulence strains). Although a protein entry receptor has not yet been identified, carbohydrate co-receptors that effect docking and concentration of the virus on the cell surface are known for both TMEV neurovirulence groups. Low-neurovirulence TMEV use  $\alpha$ 2,3-linked *N*-acetylneuramic acid (sialic acid) on an N-linked glycoprotein, whereas high-neurovirulence TMEV use the proteoglycan heparan sulfate (HS) as a co-receptor. While the binding of low-neurovirulence TMEV to sialic acid can be inhibited completely, only a third of the binding of high-neurovirulence TMEV to HS is inhibitable, suggesting that high-neurovirulence strains use another co-receptor or bind directly to the putative protein entry receptor. Four amino acids on the surface (VP2 puff B) of low-neurovirulence strains make contact with sialic acid through non-covalent hydrogen bonds. Since these virus residues are conserved in all TMEV strains, the capsid conformation of this region is probably responsible for sialic acid binding. A persistence determinant that maps within the virus coat using recombinant TMEV is also conformational in nature. Low-neurovirulence virus variants that do not bind to sialic acid fail to persist in the central nervous system of mice, indicating a role for sialic acid binding in TMEV persistence. Analysis of high-neurovirulence variants that do not bind HS demonstrates that HS co-receptor usage influences neuronal tropism in brain, whereas, the HS

co-receptor use is not required for the infection of spinal cord anterior horn cells associated with poliomyelitis.

**Keywords** Co-receptor · Heparan sulfate · Multiple sclerosis model · Persistent infection · Picornavirus · Sialic acid · Theiler's murine encephalomyelitis virus · Viral pathogenesis

### Abbreviations

BeAn virus	low-neurovirulence TMEV strain
BHK-21	baby hamster kidney fibroblast cells
CNS	central nervous system
CHO	Chinese hamster ovary cells
CSA	chondroitin sulfate A
DA virus	low-neurovirulence TMEV strain
DS	dermatan sulfite
EMCV	encephalomyocarditis virus (related Cardiovirus)
GAG	glycosaminoglycan
GDVII virus	high-neurovirulence TMEV strain
HS	heparan sulfate
KS	keratin sulfate
Mengo virus	related Cardiovirus
PG	proteoglycan
PNGase	N linked-specific endoglycosidase
TMEV	Theiler's murine encephalomyelitis virus
UGT	UDP-galactose transporter

### Introduction

Theiler's murine encephalomyelitis viruses (TMEV) are enteric pathogens that belong to the cardiovirus genus in the family, *Picornaviridae*, and are closely related to encephalomyocarditis virus (EMCV) [1]. Isolated by Max

H.L. Lipton · A.S.M. Kumar · S. Hertzler · H.V. Reddi  
Department of Neurology and Microbiology-Immunology,  
University of Illinois at Chicago, Chicago, IL 60612-7344

Theiler in the early 1930s from mice with spontaneous paralysis [2], TMEV are known to biomedical investigators because they are ubiquitous in mice not housed under barrier conditions. In nature, TMEV are widespread in feral *Mus musculus*, and to a certain extent, in species of water voles [3]. Virus transmission occurs by the fecal-oral route, resulting in an inapparent infection of the gut. On rare occasions [4], TMEV spreads to the central nervous system (CNS), causing cytolytic infection of spinal cord anterior horn cells and flaccid hind-limb paralysis, i.e., mouse poliomyelitis [5].

Infection of mice with low-neurovirulence TMEV strains provides a highly relevant experimental animal model for multiple sclerosis in humans. Low-neurovirulence TMEV strains, such as BeAn and DA, produce a persistent infection in the mouse CNS that results in mononuclear cell inflammation and demyelination [6,7], whereas high-neurovirulence strains, such as GDVII and FA, produce a rapidly fatal encephalitis.

Virus-receptor interactions usually involve multiple steps to promote viral entry and infection. The initial step is often low-affinity binding to an attachment factor, i.e., a co-receptor, which effects docking and concentration of virus on the cell surface. This interaction is followed by binding to a high-affinity entry receptor. Viral receptors and co-receptors have been identified for a number of picornaviruses [8]. Since picornaviruses do not have an envelope that can fuse to the lipid bilayer of the cell membrane, virus entry and initiation of infection is believed to require binding to a protein entry receptor. Moreover, the presence of a 25 Å-deep depression on the cardiovirus surface, analogous to the canyon on polioviruses and rhinoviruses, suggests that cardioviruses require a protein entry receptor [9,10]. A TMEV protein entry receptor has not yet been identified, but members of both neurovirulence groups bind to a 34-kD membrane protein in a ligand binding assay [11]. However, low-neurovirulence TMEV use  $\alpha$ 2,3-linked *N*-acetylneuramic acid on an N-linked glycoprotein as a co-receptor [12,13], whereas the high-neurovirulence GDVII uses the proteoglycan (PG) heparan sulfate (HS) as a co-receptor [14].

#### UDP-galactose transporter is required for TMEV entry into mammalian cells

In the late 1990s, extensive screening of mammalian cell lines failed to reveal a TMEV receptor-negative cell line, perhaps because the TMEV receptor is widely expressed in eukaryotic cells. R26, a BHK-21 cell variant selected for BeAn virus resistance and apparently “receptor-negative” [15], was generated and used in screening a BHK-21 cell cDNA library. The sequence of a clone found to mediate entry and infection by viruses of both TMEV groups in R26 cells was nearly identical to the human UDP-galactose trans-

porter (UGT), a member of the family of nucleotide-sugar transporter proteins in the Golgi involved in the biosynthesis of complex carbohydrate structures. UGT mRNA from R26 cells revealed a 496-nucleotide deletion involving the C-terminal amino acids 255 to 392 and 81 nucleotides of the 3' noncoding region predicted to alter membrane glycosylation. These results raised the possibility that UGT might mediate TMEV entry and infection by virtue of its transporter function of adding galactose to another receptor protein, or by acting as the TMEV entry receptor via UGT cycling to the cell surface. The latter possibility suggested the requirement for a specific glycoprotein interaction for GDVII virus cell binding and entry. However, polyclonal rabbit antibodies to the human UGT did not block binding or infection of mammalian cells by either high- or low-neurovirulence TMEV, and incubation of TMEV with galactose or blocking galactose on the cell surface with lectins did not inhibit binding or infection [16]. Thus, UGT is not a receptor for TMEV nor does TMEV bind directly to galactose. The requirement of UGT for low-neurovirulence BeAn virus binding and infection of cells became evident based on previous studies of the binding moiety for TMEV, which suggested that low-neurovirulence BeAn virus bound sialic acid [12], and on the fact that the penultimate sugar galactose is required for attachment of sialic acid to oligosaccharides. The need of UGT for high-neurovirulence GDVII virus binding and infection was not evident at that time.

#### Low-neurovirulence TMEV use $\alpha$ 2-3-linked sialic acid on an N-linked glycoprotein as a co-receptor

Based on the study suggesting that low-neurovirulence TMEV bind to sialic acid [12], subsequent work [13] using *Clostridium perfringens* neuraminidase clearly demonstrated a >90% reduction in BeAn virus binding to BHK-21 cells treated with the enzyme (Fig. 1A). GDVII virus binding was unaffected [13]. A typical dose-response to increasing neuraminidase concentrations was observed, with maximal inhibition at 1 mU/ml. Treatment of BHK-21 cells with *Vibrio cholerae* neuraminidase also abrogated BeAn virus binding. Neuraminidase treatment of BHK-21 cells showed a similar effect on infection by BeAn virus [13]. Moreover, mutant Chinese hamster ovary (CHO) cells deficient in the UDP-galactose transporter (Lec-1), CMP-sialic acid transporter (Lec-2), or N-linked carbohydrate processing (Lec-1) also showed >90% reduction in BeAn virus binding (Fig. 1B) and infection (not shown). The modest reduction observed in GDVII virus binding, but not infection, is discussed below.

Analysis of genetically deficient cell lines (glycolipid-deficient GM95 cells and N-linked, O-linked, and

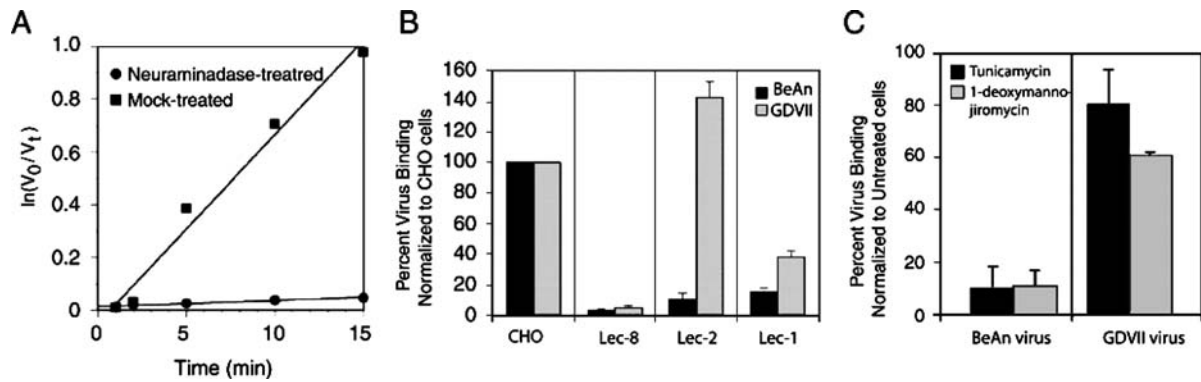


**Fig. 1** (A) BeAn virus binding to BHK-21 cells as measured by radiolabeled virus association. Purified  $^{35}\text{S}$ -labeled BeAn virus ( $1 \times 10^6$  cpm) was incubated with  $1 \times 10^6$  BHK-21 cells at  $4^\circ\text{C}$  for varying times and washed extensively. BHK-21 cells were treated with 1 mU/ml of *Clostridium perfringens* neuraminidase for 45 min at  $37^\circ\text{C}$  (●) or mock-treated (■). Cell-associated radioactivity was measured with a scintillation counter and plotted:  $V_0$  is the total amount of virus particles added to  $1 \times 10^6$  cells;  $V_t$  is the unattached virus at a given time point. (B) BeAn and GDVII virus binding to Lec cell mutants. Virus binding was measured by flow cytometry and compared to binding of

lipid-linked glycosylation-deficient ldlD cells) and metabolic inhibitors indicated that neither BeAn nor GDVII virus required glycolipids or O-linked carbohydrates for cell surface attachment and infection [13]. To further analyze the role of N-linked glycosylation in TMEV binding and infection, BHK-21 cells were treated with tunicamycin, a fungal toxin that blocks assembly of *N*-acetylglucosamine on the lipid carrier dolichol phosphate, or with 1-deoxymannojirimycin, which blocks processing by  $\alpha$ -mannosidase I [17,18]; both toxins inhibit early steps in the assembly of N-linked carbohydrates. BeAn virus binding to cells treated with either toxin was decreased by more than 90%, whereas GDVII virus binding was reduced by only 20–35% (Fig. 1C). In contrast, no inhibition of GDVII virus infection was observed in cells treated with these metabolic inhibitors. Further analysis of the role of N-linked oligosaccharides in BeAn virus binding using cell membrane extracts digested with varying concentrations of PNGase F [19] or neuraminidase, blotted onto nitrocellulose filters and overlaid with S-labeled BeAn virus revealed abrogation of BeAn virus binding to membrane extracts digested with either enzyme. Digestion with O-glycanase could not be carried out because prior treatment with neuraminidase is required for enzymatic activity [19]. Collectively, these results indicated that the sialic acid moieties important for BeAn virus attachment and infection are found on N-linked glycoproteins, whereas N-linked glycoproteins probably account for only a minor portion of GDVII virus binding. Evidence that low-neurovirulence TMEV bind specifically to  $\alpha$ 2-3-linked sialic acid moieties came from the demonstration that incubation of low-neurovirulence BeAn virus with  $\alpha$ 2-3-sialyllactose, but not  $\alpha$ 2-6-sialyllactose, strongly inhibited binding and infection

parental CHO cells. Lec-2 and Lec-8 cells have defects in the CMP sialic acid and UDP galactose transporters, respectively, while Lec-1 cells are defective in N-linked carbohydrate processing. Data are given as % mean fluorescence intensity  $\pm$  sd. (C) BeAn and GDVII virus binding to BHK-21 cells treated with tunicamycin or 1-deoxymannojirimycin. Cells were grown in medium containing  $20 \mu\text{g/ml}$  of tunicamycin or 1-deoxymannojirimycin for 48 hr before virus was added. Virus binding was measured by flow cytometry, and mean fluorescence intensity  $\pm$  sd was determined by comparison with untreated cells

of BHK-21 cells [20]. Together, these findings suggest that low-neurovirulence TMEV bind to a specific sialic acid present on an N-linked glycoprotein, which may be the TMEV protein entry receptor.

### Low-neurovirulence TMEV contact three virus residues on VP2 puff B and another nearby residue

The crystal structure of the low-neurovirulence DA virus in complex with sialyllactose was resolved to  $3 \text{ \AA}$ , revealing three VP2 amino acids on puff B (Q2161, A2163 and G2174)<sup>1</sup> and one VP3 residue (Q3232), all within a positively charged area on the viral surface, that make contact with sialic acid (and not the penultimate sugar galactose) through non-covalent hydrogen bonds (Fig. 2A and B) [21]. Since these four viral residues are conserved in all TMEV (two high- and six low-neurovirulence capsid sequences are known), and the largest difference in root-mean-square deviation between the  $\text{C}\alpha$  coordinates of viruses of the two neurovirulence groups lies in VP2 puff B [22], the capsid conformation of this region in the low-neurovirulence strains is probably responsible for sialic acid binding.

Of the three VP2 residues that contact sialic acid, Q2161 uses its side chain, whereas A2163 and G2174 use their main chain carbonyl oxygen and amide, respectively. Thus, substitutions at Q2161 are more likely than those at A2163 or G2174 to disrupt the interaction with sialic acid. BeAn

<sup>1</sup>By convention, the first digit designates the picornavirus capsid protein (VP1, VP2, VP3 or VP4) and the remaining three digits, the amino acid position.

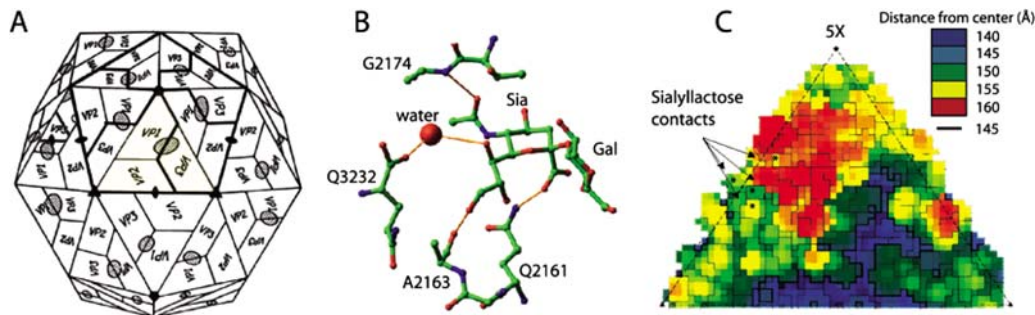


**Fig. 2** (A) Diagram of the icosahedral shell structure of a cardiovirus. The virion is composed of 12 pentamers, each of which has five protomers composed individually of four capsid proteins VP1, VP2, VP3 (exposed on the virion surface) and VP4 (buried beneath VP2 next to the virion RNA). The virion surface contains 25 Å-deep receptor binding depressions (oval hatched areas) that span residues at the junction of VP1 and VP3. A single pentamer and one of its protomers are highlighted by darker lines. The yellow shading denotes an asymmetrical

icosahedral unit. (B) DA residues involved in sialic acid binding by either forming hydrogen bonds with sialic acid (G2174, A2163 and Q2161) or through a water molecule (Q3232). Sia, sialic acid; Gal, galactose. (C) Two-dimensional map of residues that shape the DA outer surface within one asymmetric icosahedral unit. Distances from the residues to the virion center are color-coded according to the legend (upper right). Arrows indicate the location of the four virus residues that bind sialic acid on the VP2 puff B elevation

residue Q3232, which contacts sialic acid, is part of the VP3–VP1 cleavage dipeptide and cannot be mutated. To systematically test the importance of these sialic acid-binding residues in viral entry and infection, the VP2 puff B amino acids were mutated in a viral subclone assembled into a full-length infectious BeAn virus clone, and the consequences of these single amino acid substitutions on sialic acid binding were analyzed in a biological context as it is expressed on complex carbohydrate moieties at the cell surface [23]. The data indicated direct involvement of BeAn virus residues Q2161 and G2174 in viral attachment to sialic acid expressed on mammalian cells and erythrocytes. Mutations at these sites resulted in loss of or reduced viral binding and hemagglutination, and in the inability of the mutant viruses to spread among BHK-21 cells. Mutant viruses at A2163 showed no evidence of replication in BHK-21 cells following electroporation, reflecting a defect in polyprotein processing observed in *in vitro* translation of transcribed RNA. Thus, mutations at Q2161 and G2174 are, in effect, lethal mutations in BeAn virus since they disrupt the first step in the viral life cycle, binding to host cells.

### Low-neurovirulence TMEV binding to sialic acid co-receptor(s) is required for persistent infection of mice

Adami *et al.* [24] mapped a determinant for TMEV persistence within the capsid by analysis of recombinant viruses constructed using high- and low-neurovirulence TMEV sequences. The results suggested that the persistence determinant was conformational, requiring homologous sequences in the VP2 and VP1 loops which interact on the virion surface. Since the capsid conformation of the VP2 puff B in the low-neurovirulence strains appears to be responsible for

sialic acid binding, we asked whether a low-neurovirulence TMEV that did not use sialic acid as a co-receptor would retain the ability to cause persistent infections. To generate a DA virus that did not use binding to sialic acid for infection, the parent virus was passed in Lec-2 cells, which lack the CMP sialic acid transporter and cell surface sialic acid [25]. DA virus was used because of the availability of the original brain-derived virus stock that had never been passed in cell culture. Sialic acid dependence for infection was indicated by formation of only small foci of cpe after day-7 pi, minimal progression of cpe on passage 1 (P1), and the requirement for two additional passages to achieve complete cpe, i. e., at  $\geq$ P3 (Fig. 3A). The P3 virus had a single mutation, G1100D, on VP1 loop II, while the P5-adapted virus used in the following studies had two additional amino acid substitutions, T1081I, and T3182A, on VP1 loop I and the VP3 GH loop (2nd corner), respectively (Fig. 3B). The VP1 mutations were in surface loops that interact through non-covalent bonds with VP2 puff B, the site of sialic acid binding, while the VP3 mutation was in a flexible loop adjacent to the pit (Fig. 3B), termed the “receptor binding loop” in the related Mengovirus [26].

The adapted virus no longer used sialic acid as a co-receptor, and showed increased acute CNS virulence (Fig. 3C), but viral copy numbers were dramatically reduced ( $>10^6$ -fold) (Fig. 3D) and white matter inflammation and demyelination in the spinal cord were significantly reduced at 55 days pi [25]. A role for VP1 loop II residue, G1100D, in sialic acid binding and CNS persistence was demonstrated by analysis of a DA infectious cDNA clone with this mutation (Fig. 3C, D). Infectious cDNA DA virus was derived from *in vitro* RNA transcription of a full-length DNA clone with the G1100D mutation after transfection of BHK-21 cells; in this instance the parental virus was derived from the parental DA virus clone. Loss of CNS persistence in mice also



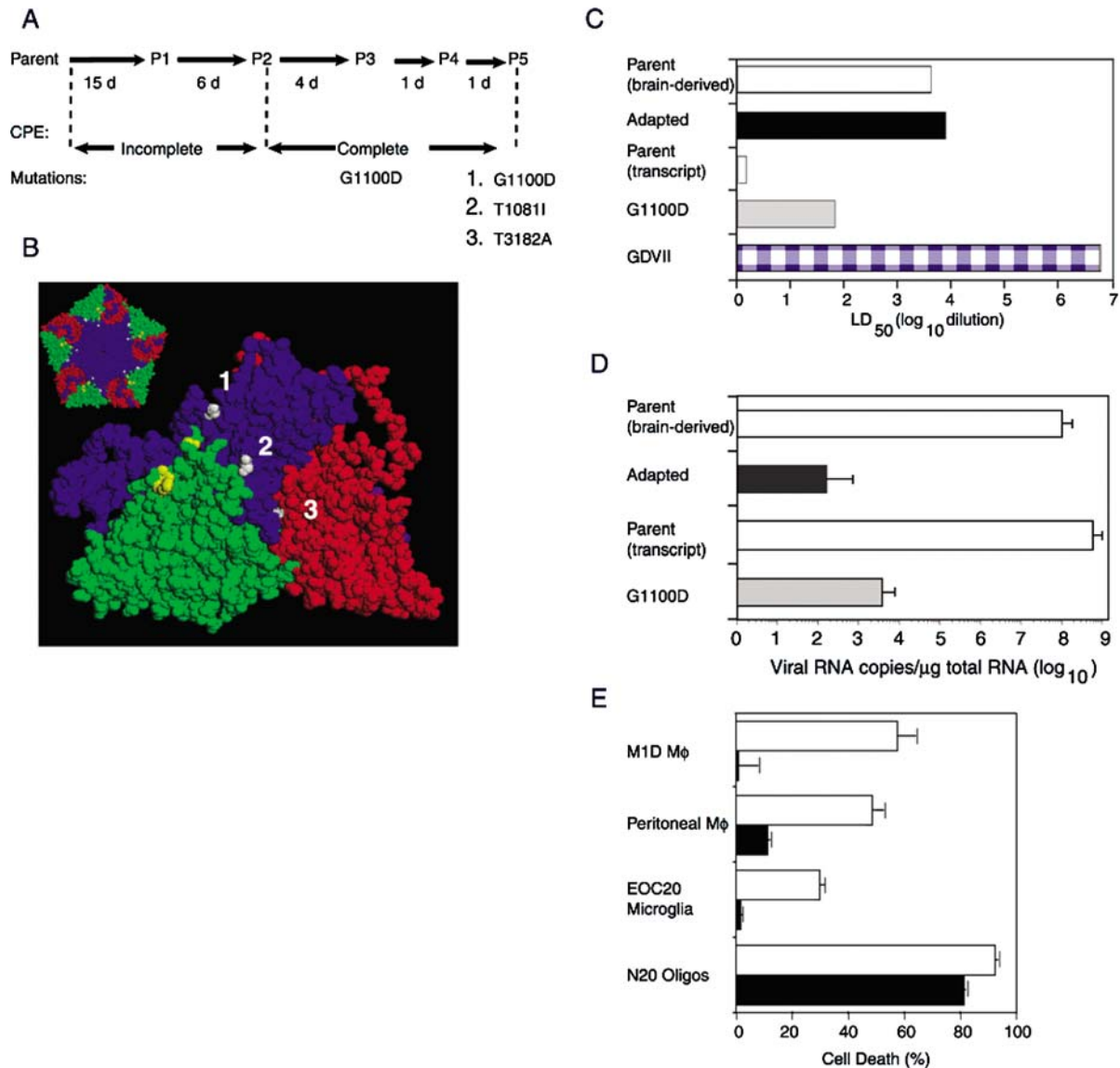


**Fig. 3** (A) Passage history of low-neurovirulence brain-derived DA virus adapted to grow in Lec-2 cells, lacking sialic acid. Number of days of each passage, relative extent of cpe, and mutations in the L-P1 genomic regions are shown. (B) Image of DA virus asymmetric icosahedral unit (“protomer”) generated by the RasMol program: blue, VP1; green, VP2; red, VP3; yellow, sialic acid binding residues; and white, DA virus adaptation mutations. Inset (upper left) shows a pentamer. Numbers 1, 2 and 3 correspond to the mutations designated in (A). (C) Effect of sialic acid-independent DA virus infection on acute CNS virulence. LD<sub>50</sub> determinations in adult CD-1 mice show that the virulence of adapted DA virus was comparable to that of the parental virus, while G1100D was more virulent than its parental virus (see text for the difference between parental brain-derived and transcript-derived viruses). The LD<sub>50</sub> of high-neurovirulence GDVII virus is shown for comparison.

correlated with a significant reduction in infection of murine macrophages, but not oligodendrocytes, *in vitro* (Fig. 3E).

Several mechanisms might explain TMEV persistence after sialic acid-dependent infection: (1) sialic acid allows TMEV binding and infection of macrophages, which is

son. Because the brain-derived DA parental virus cannot be assayed by plaqueing, pfu/LD<sub>50</sub> could not be determined. (D) Effect of sialic acid-independent DA (adapted) virus infection on CNS persistence. Spinal cord genome copy numbers determined by real-time RT-PCR at day 55 were significantly reduced in adapted virus- compared to brain-derived parental virus-infected mice ( $n = 14$  in each group) ( $P < 0.0001$ ), as well as in G1100D mutant virus- compared to transcript-derived parent virus-infected mice ( $n = 4$  in each group) ( $P = 0.0286$ ). (E) Cell death (cpe) of murine M1D macrophages (24 h pi), peritoneal macrophages (48 h pi), EOC20 microglia (72 h pi) and N20 oligodendrocytes (24 h pi). A significant reduction in cpe was observed in M1D macrophages and peritoneal macrophages ( $P < 0.0001$ ) as well as EOC20 microglia ( $P < 0.05$ ), but not in N20 oligodendrocytes infected with adapted virus (■) compared to parent virus (□)

required for persistence; (2) access of TMEV-specific antibodies to TMEV bound to the sialic acid layer on the surface of most cells is sterically hindered; and (3) sialic acid binding enables axonal transport of TMEV from anterior horn cells in gray matter to white matter, the site of myelinated

axons. Low-neurovirulence TMEV replicate preferentially in CNS macrophages/microglia during persistence, although oligodendrocytes and astrocytes are also infected [27–29]. Experiments in which peripheral macrophages were depleted with mannosylated liposomes revealed a loss of DA virus persistence in 70% of mice [29], directly implicating a role for macrophages in TMEV persistence and suggesting a model of TMEV persistence involving macrophage-to-macrophage spread of virus with restriction of virus replication in macrophages that undergo apoptosis [30]. Host anti-viral immune responses also restrict persistence by limiting dissemination of TMEV to other cells, including oligodendrocytes, where the infection is highly cytolytic and productive. The DA adapted virus was inefficient in infecting murine macrophages but not oligodendrocytes in culture (Fig. 3E); however, further studies are needed to exclude the other mechanisms for curtailing TMEV persistence.

### High-neurovirulence TMEV strain GDVII binds to an HS co-receptor

The UDP-galactose transporter found in the trans-Golgi apparatus was shown to be required for GDVII virus binding and infection of a “receptor-negative” BHK-21 cell variant [31], pointing to the need for galactose in this process. Analysis of the role of various cell surface glycoconjugates containing galactose in binding and infection indicated that GDVII does not use either O-linked oligosaccharides or glycolipids for binding and infection, although attachment to N-linked

oligosaccharides accounted for a portion of GDVII binding [13]. Since galactose is also a component of the tetrasaccharide linker of PGs, and since HS PG are co-receptors/attachment factors for a large number of RNA and DNA animal viruses [32], including the picornaviruses echovirus-7 [33], foot-and-mouth disease virus (FMDV) [34,35], coxsackievirus B3 [36] and swine vesicular disease virus [37], we tested whether HS plays a role in GDVII virus binding and infection of mammalian cells.

### Soluble HS inhibits GDVII virus binding and infection

If GDVII infection is initiated through interaction with cell surface PGs, at least the major glycosaminoglycans (GAGs) found on membrane-associated PGs should act as a competitive inhibitor. To examine the ability of soluble GAGs to block binding and infection, respectively, GDVII virus was incubated with HS, heparin, chondroitin sulfate A (CSA), keratin sulfate (KS) and dermatan sulfate (DS) at a concentration of 250  $\mu\text{g/ml}$  before binding and infection of CHO cells at an moi of 100. Soluble CSA, KS and DS showed no inhibitory effect on GDVII virus binding and infection (Fig. 4A and B), even at a concentration of 1000  $\mu\text{g/ml}$ , whereas, 250  $\mu\text{g/ml}$  of heparin inhibited binding by 6% and infection by 30%, and 250  $\mu\text{g/ml}$  of HS inhibited binding by 25% and infection by 100%. When GDVII virus was incubated with lower concentrations of HS, a dose-response for binding and infection was observed; 1000  $\mu\text{g/ml}$  of HS inhibited GDVII virus binding by 40%, whereas 3.75  $\mu\text{g/ml}$  of HS provided

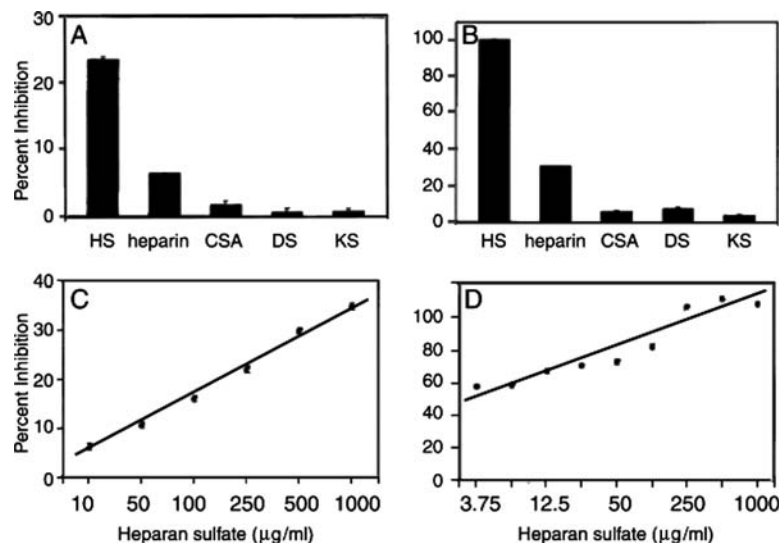


**Fig. 4** Competitive inhibition of GDVII virus binding (A) and infection (B) by GAGs. GDVII virus at an moi of 100 was incubated with 250  $\mu\text{g/ml}$  of the indicated GAG for 1 h at 37 °C, and the mixture absorbed to CHO cells. Bound virus was analyzed using flow cytometry and cpe by MTT assay at 24 h pi. Infections were carried out in 96-well plates in quadruplicate with uninfected or infected cells (with no treatment) as controls. Viability of cells was calculated as a percentage of uninfected cell controls, and percent protection was the difference in viability af-

ter infection with and without treatment. Inhibition of binding (A) and protection of cell monolayers (B) was calculated relative to binding and infection in the absence of GAGs. Data are given as mean  $\pm$  sd of 3 independent experiments. (C,D) Dose-dependent inhibition of GDVII virus binding (C) and infection (D) by soluble HS. GDVII virus was preincubated with increasing concentrations of HS, and binding and infection of CHO cells were analyzed

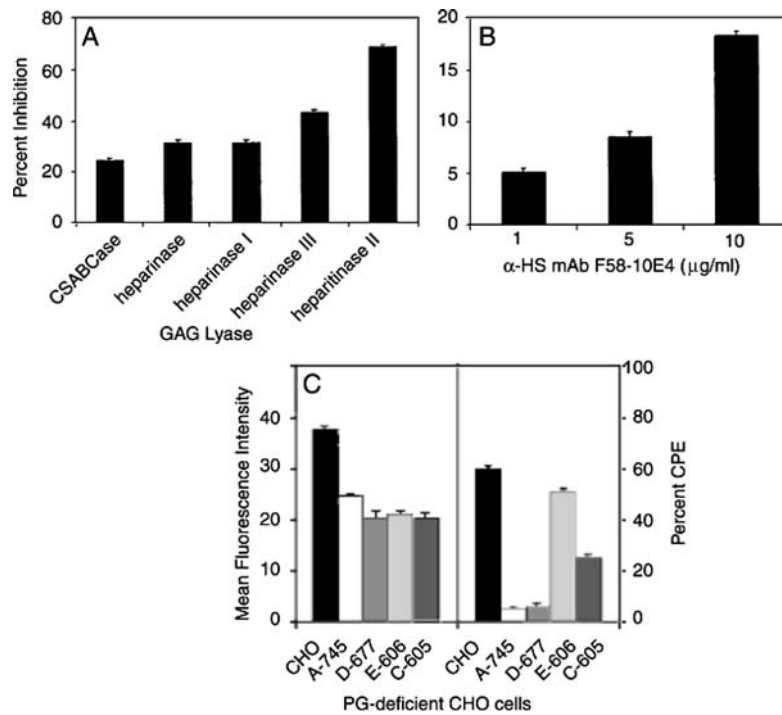


**Fig. 5** Inhibition of GDVII virus infection by pre-treatment of CHO cells with GAG lyases (A) and anti-HS antibody (B). (A) CHO cells were pre-treated with 1 U of chondroitinase ABC or 0.02 U of heparinase, heparitinase II, heparinase I or heparinase III for 1 h at 37°C prior to GDVII virus infection (moi = 100). CPE was determined by MTT assay at 24 h pi and expressed as percent inhibition. (B) CHO cells were pre-incubated with increasing concentrations of anti-HS (F58-10E4) for 1 h at 37°C prior to virus infection, and percent inhibition was determined. Data are given as mean  $\pm$  sd for 4 independent experiments. (C) Resistance of PG-deficient CHO cells to GDVII virus infection.

Selected PG-deficient mutant CHO cells were examined for GDVII virus binding (left frame) and infection (right frame). Virus was bound to CHO and PG-deficient pgsA-745 and pgsD-677 cells and undersulfated pgs E-606 and pgs C-605 cells, analyzed using flow cytometry, and plotted as mean fluorescence intensity. Percent CPE of infected CHO, PG-deficient pgs A-745 and pgsD-677, and undersulfated pgsE-606 and pgsC-605 cells was determined by MTT assay and calculated based on viability of uninfected cells at 24 hr pi. Data are given as mean  $\pm$  sd for 4 independent experiments

60% protection of monolayers (Fig. 4C and D). The inhibition was not due to interaction with CHO cells, since incubation of the cells with increasing concentrations of HS, followed by extensive washing and infection with GDVII virus at an moi of 100, did not inhibit infection. These data indicate that soluble HS has a more profound inhibitory effect on GDVII virus infection than on binding, and suggests that the effect of soluble HS is due to its direct binding by the virus.

#### GDVII virus requires cell surface HS for infection

HS is known to bind to specific cell surface receptors, e.g. those of cytokines, growth factors and chemokines [38], raising the possibility that the observed effects of soluble HS reflect competition for a common receptor rather than direct binding to virus. Because the greatest effect of soluble HS was on infection, we analyzed GDVII virus infection of cell monolayers incubated with: heparinase, which cleaves the  $\alpha$ -glucosaminide linkage to 2-*O*-sulfo-L-iduronic acid; heparinase I, which cleaves the 1-4-linked D-glucuronate or L-iduronate residues in heparin; heparinase III (heparitinase I), which eliminates sulfate and cleaves

$\alpha$ -*N*-acetyl-D-glucosaminidic linkages in HS; heparitinase II, which cleaves the  $\alpha$ -*N*-acetyl-D-glucosaminidic linkages in HS and heparin; and chondroitinase ABC, which cleaves N-acetylhexosaminide linkages in all chondroitin sulfates. The two enzymes that act on HS, heparitinase II and heparinase III, showed the greatest inhibition of infection, whereas cells pre-incubated with heparin-specific enzymes heparinase and heparinase I showed only slightly greater inhibition of infection than did chondroitinase ABC digestion (Fig. 5A). These data further support a role for HS in GDVII virus infection. Finally, infection at an moi of 100 was blocked with 1 to 10  $\mu$ g/ml of anti-HS monoclonal antibody F58-10E4, resulting in partial protection from infection (Fig. 5B). Presumably, higher antibody concentrations would have resulted in even greater protection.

#### PG-deficient CHO mutants are resistant to infection by GDVII virus

CHO cell mutants deficient in GAG synthesis were used to further define the role of HS and its component molecules in GDVII virus binding and infection. Mutant pgsA-745 lacks

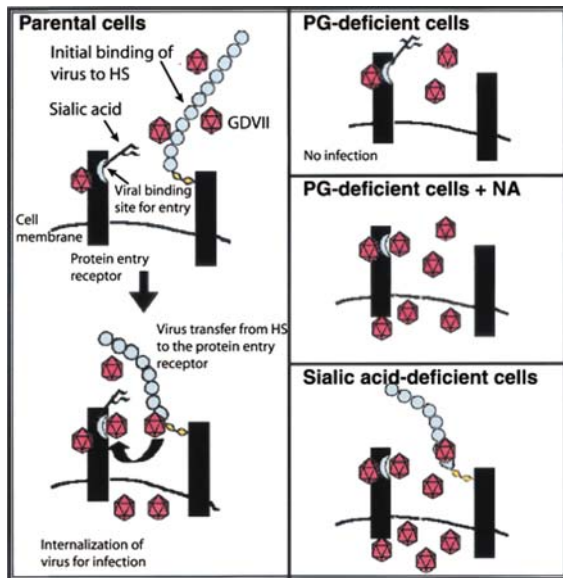


**Fig. 6** A model for two components of GDVII virus binding and subsequent internalization by a protein entry receptor. (Left) GDVII virus binds to HS which mediates internalization via a protein entry receptor to infect parental CHO, BHK-21 and other mammalian cells. Note that GDVII virus can also bind directly to the protein entry receptor, but infection is sterically hindered by sialic acid moieties located on the protein entry receptor. (Right) Top panel: GDVII virus is unable to infect PG-deficient cells lacking HS. Although the virus binds directly to the protein entry receptor, steric hindrance by sialic acid blocks virus internalization. Middle panel: Removal of sialic acid from PG-deficient cells with neuraminidase permits viral access to the protein entry receptor, and thereby infection. Bottom panel: Binding and infection of GDVII virus of Lec-2 cells, which have HS but lack cell surface sialic acid, is even more efficient than in the other cells

xylosyl transferase, an enzyme required for initiation of the synthesis of GAGs, and produces no detectable levels of GAGs [39]; pgsD-677 lacks galactosyl transferase I and is deficient in the ability to add HS disaccharide chains to the tetrasaccharide linker [40]; pgsE-606 is partially defective in *N*-sulfotransferase activity; pgsC-605 completely lacks sulfate transporter activity; and pgsE-606 and pgsC-605 synthesize undersulfated HS. While only a modest reduction in GDVII virus binding was observed in pgsA-745 and pgsD-677 cells (not shown), infection in these mutants was markedly reduced (Fig. 5C). Infection was also reduced in pgsC-605, and to a much lesser extent in pgsE-606 cells, indicating that the degree of sulfation is an important factor in GDVII virus infection. Binding or infection of BeAn virus was shown to be not affected in any of the cells deficient in GAG synthesis, confirming that HS is used only by the high-neurovirulence TMEV [14].

Neuraminidase treatment of CHO cell mutants restores GDVII infection

GDVII virus binding and infection of Lec-2 cells, a CHO cell mutant lacking the CMP sialic acid transporter, was sig-

**Table 1** Classification of cardiomyoviruses into two groups and TMEV according to neurovirulence

Group A (EMCV)	Group B (TMEV)
EMCV	GDVII*
Mengo	Ask-1*
	DA <sup>+</sup>
	BeAn <sup>+</sup>

\*High-neurovirulence group

<sup>+</sup>Low-neurovirulence group

nificantly higher than to parental cells, suggesting that the removal of sialic acid from the cell surface allows direct access of GDVII virus to the putative protein entry receptor [14]. In fact, GDVII virus binding to pgsA-745 and -D-677 cell monolayers treated with neuraminidase at a concentration that completely abrogated BeAn virus binding increased by 0.8 to 2-fold, comparable to binding levels observed with parental cells. Further, removal of cell surface sialic acid rendered these mutant cells permissive to GDVII virus infection [14].

Based on retained binding and lack of infection observed in PG-deficient cells, we postulate that GDVII virus binding has two components: HS binding and direct binding to a protein entry receptor. Infectivity in HS-deficient CHO cells is restored by removal of cell surface sialic acid with neuraminidase, suggesting that sialic acid sterically hinders full access to the protein entry receptor required for infection. Consistent with this notion, BeAn virus binds sialic acid and can competitively inhibit GDVII virus binding, whereas GDVII virus does not inhibit BeAn virus binding [12]. Based on our data, we propose a model wherein high- and low-neurovirulence TMEV bind different attachment factors, *e.g.* HS and sialic acid, but use a common protein entry receptor. Figure 6 depicts the proposed model of infection for the high-neurovirulence TMEV.

### GDVII HS co-receptor use influences range of neuronal infection in the mouse CNS

The interaction between high-neurovirulence TMEV and its co-receptor was further studied using GDVII virus adapted to PG-deficient cells [41]. To generate a high-neurovirulence TMEV that did not require binding to HS, GDVII virus was passed in CHO mutant pgsA-745 cells deficient in xylosyl transferase [42], an enzyme required for attachment of the tetrasaccharide linker to the protein core and for GAG synthesis. Unlike the complete cpe at 48 h pi observed in parental CHO cells, cpe of the passed virus was only observed after day-3 pi and was complete on day-5 pi. Two additional



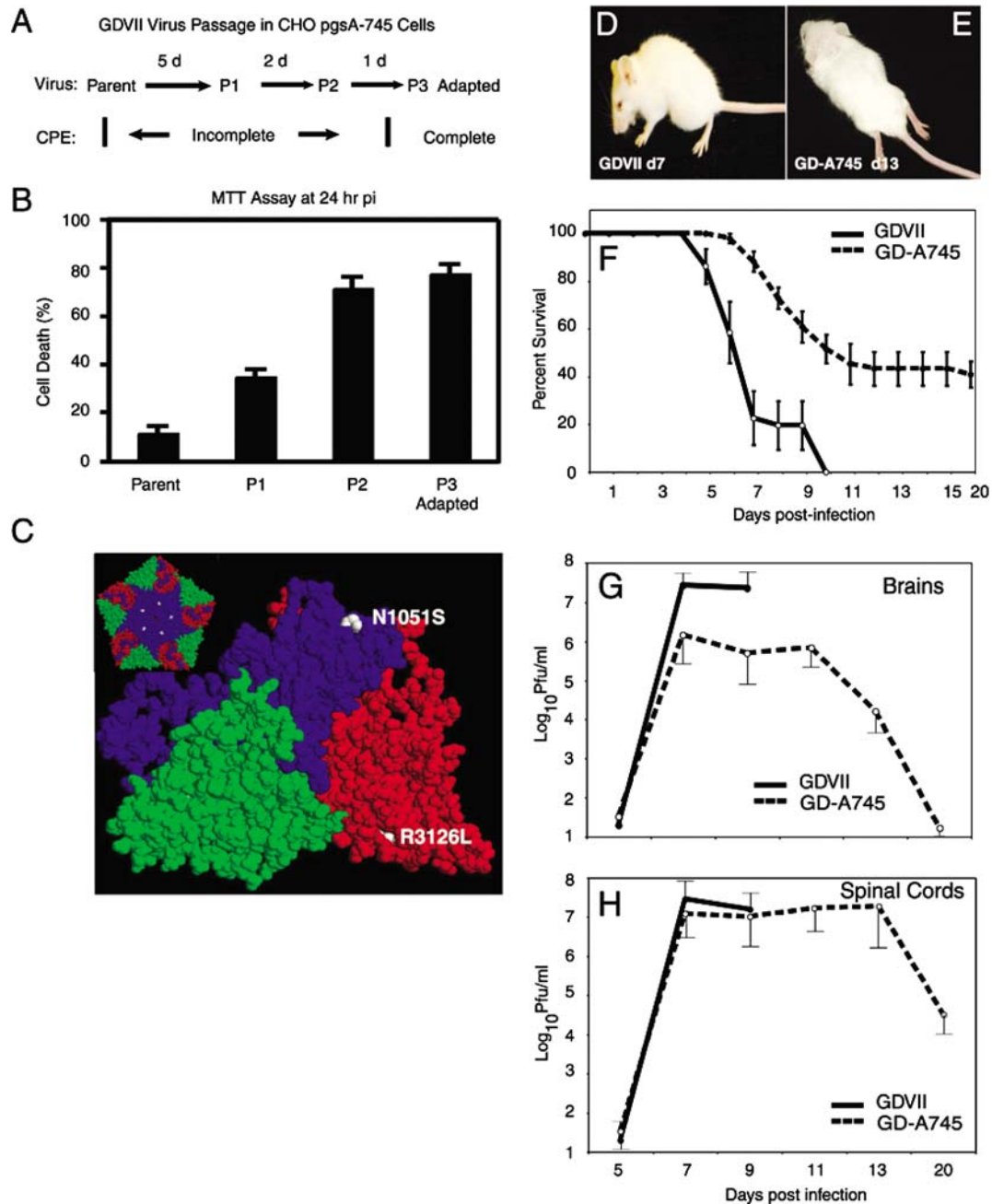


**Fig. 7** (A) Adaptation of GDVII virus to PG-deficient cells. pgsA-745 cells were infected with GDVII (moi of 10) and allowed to progress to maximal cpe reached at 5 days pi (P1). Lysates were passed twice more in pgsA-745 cells until ~90% cpe was obtained within 24 h pi (P3). (B) Cytopathic effect induced at different passages determined in MTT assay, with cell death calculated as percent (mean ± sd of 4 independent experiments) of uninfected controls. (C) Mutations in GD-A745 on the GDVII asymmetric icosahedral unit (protomer) in a space-filling model

passages were required for >90% cpe to develop within 24 h, *i.e.*, at P3, and a stock of virus was prepared (Fig. 7A and B).

The adapted virus, designated GD-A745, acquired two mutations (R3126L, N1051S), both on surface loops in the capsid (Fig. 7C) [41]. GD-A745 no longer used HS for bind-

ing and entry, and infectious virus yields in mammalian cells were 25-fold higher for the adapted virus compared to the parental GDVII virus in BHK-21 cells [41]. Disease pathogenesis was analyzed in 5- to 6-week-old CD-1 mice inoculated ic with 100 pfu of GDVII or GD-A745 viruses [41].

LD50 determinations indicated that GD-A745 virus was 5-fold less virulent than GDVII virus (pfu/LD50 were 32 and 6, respectively). GDVII virus-infected mice developed signs of encephalitis by day 5 pi and all animals died by days-9 to 11 pi. In contrast, GD-A745 virus-infected mice developed flaccid limb paralysis without signs of encephalitis, and ~40% of mice survived to day 20 pi (Fig. 7D–F). All mice infected with 1000 pfu of GD-A745 virus died by day 15 pi with flaccid paralysis but without signs of encephalitis.

Virus growth in brain peaked at day 7 pi in mice infected with 100 pfu of either virus; however, titers were ~20-fold higher in GDVII virus- than in GD-A745 virus-infected mice on days 7 and 9 pi (Fig. 7G). Initial kinetics of virus growth in spinal cords of mice infected with either virus was similar, with peak titers at day 7 pi (Fig. 7H). Spinal cord virus titers plateaued after day 7 pi in GD-A745-infected mice, in contrast to brains where titers steadily declined.

Virus antigen staining of brain sections revealed numerous focal areas of positive cells (mostly neurons based on morphology) in the neocortex, hippocampal pyramidal cell layer and brainstem of GDVII-infected mice, but positive cells were only rare in the brainstem and absent in the cerebral hemispheres of GD-A745-infected mice on days 7–9 pi [41]. Spinal cords of mice infected with GDVII virus contained extensive numbers of virus antigen-containing neurons in both the anterior and posterior gray matter, whereas infected neurons, generally fewer in numbers were observed only in the anterior gray matter of GD-A745-infected mice. Histopathology sections revealed consistently more severe pathologic changes (neuronophagia, astrocytosis, microglial proliferation, and mononuclear cell infiltration in perivascular sites and leptomeninges) in the neocortex, hippocampus and brainstem of GDVII- than GD-A745-infected mice on days 7–9 pi. However, such changes in spinal cord gray matter were more severe in GD-A745- than GDVII-infected mice. Poliomyelitis in GD-A745 spinal cords progressed between days 9 and 13 pi.

Together, these results indicate that GDVII with abrogated HS co-receptor useage show attenuated neurovirulence and changed cell tropism, essentially limiting infection to neurons in the anterior gray matter of the spinal cord. Attenuation of brain infection allowed host survival past day-11 pi (the longest survival of parental virus-infected mice) and expression of clinical poliomyelitis in the mutant-infected mice. The same analyses carried out using GDVII adapted to growth in another proteoglycan-deficient cell line, pgsD-677, which lacks only HS but not other GAGs, gave similar results. The adapted GD-D677 virus was virtually identical to GDA745 with respect to capsid mutations, virus yields in BHK-21 and Lec-2 cells, and attenuation of neurovirulence in mice (not shown). Thus, use of HS as a co-receptor by GDVII virus facilitates cell entry and plays an important role in cell tropism and neurovirulence *in vivo*.

Indications of regional differences in HS expression in the CNS [43, 44] raise the possibility that GDVII infection is more dependent on specific HS binding in some sets of neurons, e.g., those in the lower layers of the neocortex, hippocampal pyramidal layer, brainstem and posterior spinal cord gray matter, than in other sets, e.g., anterior horn cells. Other uninfected neurons may not express HS at all. Further studies of specific brain regions will help to elucidate the role of HS use in GVII infection.

## Concluding remarks

Infection of mice by low- or high-neurovirulence TMEV strains provides relevant experimental animal models for acute encephalitis and for persistent infection leading to chronic demyelinating disease (multiple sclerosis). Members of both neurovirulence groups bind to carbohydrate co-receptors that effect docking and concentration of the virus on the cell surface for infection of mammalian cells. The available evidence indicates that use of sialic acid and HS co-receptors is a major determinant of which cells in the mouse CNS become infected. Further knowledge of the interaction of TMEV with its co-receptors promises to shed light on the pathogenesis of viral encephalitis and multiple sclerosis.

## References

1. Pevear, D.C., Calenoff, M., Rozhon, E., Lipton, H.L.: Analysis of the complete nucleotide sequence of the picornavirus Theiler's murine encephalomyelitis virus indicates that it is closely related to cardioviruses. *J. Virol.* **61**, 1507–1516 (1987)
2. Theiler, M.: Spontaneous encephalomyelitis of mice - a new virus disease. *Science*. **80**, 122 (1934)
3. Lipton, H.L., Kim, B.S., Yahikozawa, H., Nadler, C.F.: Serological evidence that *Mus musculus* is the natural host of Theiler's murine encephalomyelitis virus. *Virus Res.* **76**, 79–86 (2001)
4. Olitsky, P.K.: Viral effect produced by intestinal contents of normal mice and those having spontaneous encephalomyelitis. *Proc. Soc. Exp. Biol. Med.* **43**, 434–437 (1939)
5. Theiler, M.: Studies on poliomyelitis. *Medicine*. **20**, 443–462 (1941)
6. Lipton, H.L.: Theiler's virus infection in mice: An unusual biphasic disease process leading to demyelination. *Infect. Immun.* **11**, 1147–1155 (1975)
7. Lehrich, J.R., Arnason, B.G.W., Hochberg, F.H.: Demyelinating myelopathy in mice induced by the DA virus. *J. Neurol. Sci.* **29**, 149–160 (1976)
8. Rossmann, M.G., He, Y., Kuhn, R.J.: Picornavirus-receptor interactions. *Trends Microbiol.* **10**, 324–331 (2002)
9. Rossmann, M.G., Arnold, E., Erickson, J.W., Frankenberger, E.A., Griffith, J.P., Hecht, H.-J., Johnson, J.E., Kamer, G., Luo, M., Mosser, A.G., Rueckert, R.R., Sherry, B., Vriend, G.: Structure of a human common cold virus and functional relationship to other picornaviruses. *Nature*. **317**, 145–153 (1985)
10. Hogle, J.M., Chow, M., Filman, D.J.: Three-dimensional structure of poliovirus at 2.9 Å resolution. *Science*. **229**, 1358–1365 (1985)

11. Kilpatrick, D.R., Lipton, H.L.: Predominant binding of Theiler's viruses to a 34-kilodalton receptor protein on susceptible cell lines. *J. Virol.* **65**, 5244–5249 (1991)
12. Fotiadis, C., Kilpatrick, D.R., Lipton, H.L.: Comparison of the binding characteristics to BHK-21 cells of viruses representing the two Theiler's virus neurovirulence groups. *Virology* **182**, 365–370 (1991)
13. Shah, A.H., Lipton, H.L.: Low-neurovirulence Theiler's viruses use sialic acid moieties on Nlinked oligosaccharide structures for attachment. *Virology* **304**, 443–450 (2002)
14. Reddi, H.V., Lipton, H.L.: Heparan sulfate mediates infection of high-neurovirulence Theiler's viruses. *J. Virol.* **76**, 8400–8407 (2002)
15. Hertzler, S., Trottier, M., Lipton, H.L.: Selection and characterization of a BHK-21 cell line resistant to infection by Theiler's murine encephalomyelitis virus due to a block in virus attachment and entry. *J. Gen. Virol.* **81**, 2485–2490 (2000)
16. Reddi, H.V., Lipton, H.L.: Galactose is needed only for expression of co-receptors used by Theiler's murine encephalomyelitis virus as the virus does not directly bind galactose or use the UDP-galactose transporter as a receptor. *J. Gen. Virol.* **84**, 845–849 (2003)
17. McDowell, W., Schwarz, R.T.: Dissecting glycoprotein biosynthesis by the use of specific inhibitors. *Biochimie.* **70**, 1535–1549 (1988)
18. Saunier, B., Kilker, R.D., Tkacz, J.S., Quaroni, A.Q., Herscovics, A.: Inhibition of *N*-linked complex oligosaccharide formation by 1-deoxynojirimycin, an inhibitor of processing glucosidases. *J Biol Chem.* **257**, 14155–14161 (1982)
19. Umemoto, J., Bhavanandan, V.P., Davidson, E.A.: Purification and properties of an endo- $\alpha$ -N-acetyl-D-galactosaminidase from *Diplococcus pneumoniae*. *J Biol Chem.* **252**, 8609–8614 (1977)
20. Zhou, L., Lin, X., Green, T.J., Lipton, H.L., Luo, M.: Role of sialyloligosaccharide binding in Theiler's virus persistence. *J. Virol.* **71**, 9701–9712 (1997)
21. Zhou, L., Luo, Y., Wu, Y., Tsao, J., Luo, M.: Sialylation of the host receptor may modulate entry of demyelinating persistent Theiler's virus. *J. Virol.* **74**, 1477–1485 (2000)
22. Luo, M., Toth, K.S., Zhou, L., Pritchard, A., Lipton, H.L.: The structure of a highly virulent Theiler's murine encephalomyelitis virus (GDVII) and implications for determinants of viral persistence. *Virology* **220**, 246–250 (1996)
23. Kumar, A.S., Kallio, P., Luo, M., Lipton, H.L.: Amino acid substitutions of low neurovirulence VP2 residues contacting sialic acid dramatically reduce viral binding and spread. *J. Virol.* **77**, 2709–2716 (2003)
24. Adami, C., Pritchard, A.E., Knauf, T., Luo, M., Lipton, H.L.: Mapping a determinant for central nervous system persistence in the capsid of Theiler's murine encephalomyelitis virus (TMEV) with recombinant viruses. *J. Virol.* **72**, 1662–1665 (1998)
25. Kumar, A.S.M., Reddi, H.V., Kung, A.Y., Dal Canto MC, Lipton, H.L.: Virus persistence in an animal model requires virion attachment to sialic acid coreceptors. *J. Virol.* **78**, 8860–8867 (2004)
26. Kim, S., Boege, U., Krishnaswamy, S., Minor, I., Smith, T.J., Luo, M., Scraba, D.G., Rossmann, M.G.: Conformational variability of a picornavirus capsid: pH-dependent structural changes of Mengo virus related to its host receptor attachment site and disassembly. *Virology* **175**, 176–190 (1990)
27. Clatch, R.J., Miller, S.D., Metzner, R., Dal Canto, M.C., Lipton, H.L.: Monocytes/macrophages isolated from the mouse central nervous system contain infectious Theiler's murine encephalomyelitis virus (TMEV). *Virology* **176**, 244–254 (1990)
28. Lipton, H.L., Twaddle, G., Jelachich, M.L.: The predominant virus antigen burden is present in macrophages in Theiler's murine encephalomyelitis virus (TMEV)-induced demyelinating disease. *J. Virol.* **69**, 2525–2533 (1995)
29. Pena-Rossi, C., Delcroix, M., Huitinga, I., McAllister, A., van Rooijen, N., Claassen, E., Brahic, M.: Role of macrophages during Theiler's virus infection. *J. Virol.* **71**, 3336–3340 (1997)
30. Jelachich, M.L., Lipton, H.L.: Theiler's murine encephalomyelitis virus induces apoptosis in gamma interferon activated M1 differentiated myelomonocytic cells through a mechanism involving tumor necrosis factor alpha (TNF- $\alpha$ ) and TNF- $\alpha$ -related apoptosis-inducing ligand. *J. Virol.* **75**, 5930–5938 (2001)
31. Hertzler, S., Kallio, P., Lipton, H.L.: UDP-galactose transporter is required for Theiler's virus entry into mammalian cells. *Virology* **286**, 336–344 (2001)
32. Bernfield, M., Gotte, M., Park, P.W., Reizes, O., Fitzgerald, M.L., Lincecum, J., Zako, M.: Functions of cell surface heparan sulfate proteoglycans. *Ann. Rev. Biochem.* **68**, 729–777 (1999)
33. Goodfellow, I.G., Siofoly, A.B., Powell, R.M., Evans, D.J.: Echoviruses bind heparan sulfate at the cell surface. *J. Virol.* **75**, 4918–4921 (2001)
34. Jackson, T., Ellard, F.M., Ghazaleh, R.A., Brookes, S.M., Blakemore, W.E., Corteyn, A.H., Stuart, D.I., Newman, J.W.I., King, A.M.Q.: Efficient infection of cells in culture by type-O foot-and-mouth disease virus requires binding to cell surface heparan sulfate. *J. Virol.* **70**, 5282–5287 (1996)
35. Fry, E.E., Lea, S.M., Jackson, T., Newman, J.W., Ellard, F.M., Blakemore, W.E., Abu Ghazaleh, R., Samuel, A., King, A.M.Q., Stuart, D.I.: The structure and function of a foot-and-mouth disease virus oligosaccharide receptor complex. *EMBO J.* **18**, 543–554 (1999)
36. Zautner, A.E., Korner, U., Henke, A., Dadorff, C., Schmidtke, M.: Heparan sulfate mediates swine vesicular disease virus attachment to the host cell. *J. Virol.* **77**, 10071–10077 (2003)
37. Escribano-Romero, E., Jimenez-Clavero, M.A., Gomes, P., Garcia-Ranea, J.A., Ley, V.: Heparan sulfate mediates swine vesicular disease virus attachment to the host cell. *J. Gen. Virol.* **85**, 653–663 (2004)
38. Park, P.W., Reizes, O., Bernfield, M.: Cell surface heparan sulfate proteoglycans: Selective regulators of ligand-receptor encounters. *J. Biol. Chem.* **275**, 29923–29926 (2000)
39. Huet, G., Kim, I., de Bolos, C., Lo-Guidice, J.M., Moreau, O., Hemon, B., Richet, C., Delannoy, P., Real, F.X., Degand, P.: Characterization of mucins and proteoglycans synthesized by a mucin-secreting HT-29 cell subpopulation. *J Cell Sci.* **108**, 1275–1285 (1996) 23
40. Lidholt, K., Weinke, J.L., Kiser, C.S., Lagemwa, F.N., Bame, K.J., Cheifetz, S., Massague, J., Lindahl, U., Esko, J.D.: A single mutation affects both *N*-acetylglucosaminyltransferase and glucuronosyltransferase activities in a Chinese hamster ovary cell mutant defective in heparan sulfate biosynthesis. *Proc. Natl. Acad. Sci. USA.* **89**, 2267–2271 (1992)
41. Reddi, H.V., Kumar, A.S.M., Kung, A.Y., Lipton, H.L. Heparan sulfate-dependent infection attenuates high-neurovirulence GDVII virus-induced. *J. Virol.* **78**, 8909–8916 (2004)
42. Bai, X., Wei, G., Sinha, A., Esko, J.D.: Chinese hamster ovary cell mutants defective in glycosaminoglycan assembly and glucuronosyltransferase I. *J. Biol. Chem.* **19**, 13017–13024 (1999)
43. Guido, D.X., Bai, X.-M., Van Der Schueren, B., Cassiman, J.-J., Van Den Berghe H. Developmental changes in heparan sulfate expression: In situ detection with mAbs. *J. Cell. Biol.* **119**, 691–975 (1992)
44. Hartman, U., Maurer, P.: Proteoglycans in the nervous system—the quest for functional roles in vivo. *Matrix Biology.* **20**, 23–35 (2001)